MODELLING AND MAPPING OF HEAVY-VEHICLE ENERGY CONSUMPTION

N. SAMSON
Undergraduate at Université Laval student in mechanical engineering starting soon a master's degree.

W. LEVESQUE
University Laval, Graduate of Université Laval, 2021. Currently doing research on the impact of rolling resistance on fuel economy of vehicles.

A. BÉGIN-DROLET
Professor of mechanical engineering at Université Laval in Canada and CEO of Instrumentation Icetek a spinoff company launched in November 2020 that commercialize an ice sensor he and his team have developed at Université Laval. His research focuses towards sustainable mechanical design as well as the development and management of intelligent objects and instruments.

J. LÉPINE
Assistant Professor at Université Laval, Canada Former research associate at the Centre for Sustainable Road Freight and the University of Cambridge Uk Obtained his Ph.D in mechanical engineering from Victoria University, Australia. His research focuses towards sustainable transport.

Abstract

One way to ease the adoption of low-GHG solutions in transport is to help fleet operators and policy makers understand the GHG emissions of their road network by presenting the energy consumption of the traffic on a map. This paper presents a tool that integrates multiple models to evaluate energy consumption of road freight vehicles and displays the results on a road map. The input of the model are the properties of the different vehicles that compose the local freight vehicles and the road network. Using these inputs and a predictive controller that mimic the driver's behavior, the speed profile of these vehicles can be modelled. The energy consumption associated with these vehicles is then calculated and mapped. The output of the program is a geolocated dataset of the energy density consumed by trucks of each analyzed road segment. The tool-structure modularity enables the change of the underlying hypothesis and analyze specific parameters of vehicle physics. The tool can be used as a platform for simulation and optimization of route planning taking into account the energy consumption.

Keywords: Green transport, Fuel consumption mapping, Vehicle modelling, Energy transition, Road network analysis, Traffic energy analysis, Vehicle electrification, Infrastructure and space planning, Energy savings and carbon emission reductions, and Efficient transport

1. Introduction

Transport is one of the main Green-House-Gas (GHG) emission contributors (International Transport Forum, 2010). In most developed countries, like Canada, decarbonizing this sector is challenging as road freight has been growing each year for the past 25 years(ECCC, 2020). Many solutions are being developed to reduce trucking-industry emissions whether it is to increase the efficiency of the vehicles or to change to low-emission energy sources (Ainalis *et al.*, 2020). However, it is important to plan the implementation of these solutions to maximize their benefits and ensure their fast adoption.

Presenting on a map the amount of energy used by heavy vehicles on main trucking routes can help to identify which roads have the highest consumption and develop solutions optimized for the network. For example, the Ministry of Transportation of Quebec (Canada), in collaboration with our research team, will be using this tool in a research project assessing the impact of pavement surfaces on the rolling resistance and their effect on energy consumption for the specific conditions of different motorways.

Another benefit of mapping vehicle energy consumption of the road network is that it quantifies the amount of energy used by most of the traffic. Consequently, it can be used to estimate the electric power needed to electrify road vehicles (Ainalis *et al.*, 2020). Different adoption scenarios can be evaluated and presented on a dynamic map. As it is mapped, it can also help policy makers to understand and evaluate different decarbonization scenarios. In other words, mapping the roads-network consumption can clarify some challenges of low-GHG emissions strategies for road vehicles and ease their implementation.

This paper presents a tool called the MapEUR (Map of Energy Use on Road) that integrates multiple models to evaluate energy consumption of trucks and displays the results on a road map. The inputs of the model are the properties of the road network and the different heavy vehicles travelling on it. Using these inputs, the speed profile of these vehicles is estimated from which the energy consumption can be calculated. The output of the model is a geolocated dataset of the energy consumption of each analyzed road segment scenario. A case study of a project commissioned by the MTQ (Ministry of Transportation of Quebec, Canada) of the effect of weather on truck fuel consumption is presented in the paper to showcase how the MapEUR can be used by policy makers.

2. Research Approach

The MapEUR approximates the vehicle energy consumption by estimating the traction force required to travel a specific road segment at a given speed. The traction force is integrated over the travel distance to provide the net energy required by the vehicle to travel this distance. The real amount of energy used can be computed by adding the engine efficiency of the vehicles. The MapEUR is designed to estimate the energy consumption of the traffic rather than a single vehicle and is primarily intended for highways and motorway simulations. The vehicle modelling is simplified by using a constant efficiency value for a specific vehicle and load. Fuel (energy) consumption comparisons of different speed highway duty cycles were made with the software Advisor (T. Markel, *et al.* 2005) which computes fuel consumption by modelling an engine map and gear changes. The maximum difference between the MapEUR and Advisor fuel-consumption calculations was 3.4%.

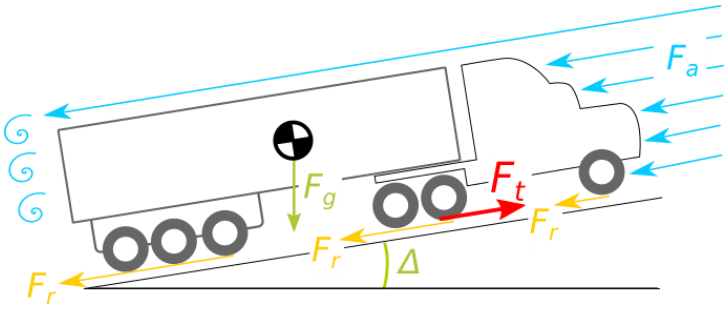

Figure 1 –Free body diagram of a vehicle; F_g is the gravity, F_r is the rolling resistance, F_t the traction force and F_a is the aerodynamic resistance.

Figure 1 presents the forces considered to estimate the traction force. The rolling-resistance force, F_r, depends on the tire, the vehicle weight and speed, road material composition, the International Roughness Index (IRI) and the pavement temperature. The rolling resistance model is detailed at section 2.3.

The aerodynamic drag force, F_a, depends on the vehicle's shape, its drag coefficient, its relative speed to the wind, and the air density. The wind speed, direction, and weather data can be downloaded from the Canadian Weather Energy and Engineering (CWEEDS, 2021), which includes 10-year data for 564 weather stations. This means that each road segment can be associated with the nearest station and the simulation can use weather data that statistically represent the location and the simulated moment of the year. The change of air density due to altitude is also considered in the simulation.

The drag coefficient also depends on the shape of the vehicle. Consequently, each combination of trucks and trailers has an impact on the drag coefficient. Even the gap between the trailer and the truck generates a variation of the drag coefficient (Mosaddeghi & Oveisi, 2015). The only way to include all these possible combinations is to define different archetypes of trucks and trailers and used them in the model. The usage of equipment to reduce the drag coefficient of trucks is also to be considered in the different vehicles archetypes (Chowdhury *et al.*, 2013). Hence, the MapEUR could be used to assess the global impact of these equipment through various scenarios.

The MapEUR is mainly used to calculate the energy consumption on highways and motorways where the speed stays close to the speed limit which is between 90 and 105 km/h in Canada. Consequently, the drag coefficient variations due to speed are negligeable (Pevitt *et al.*, 2012). Therefore, the drag coefficient used in the model is independent of the vehicle speed.

The gravitational force, F_g, depends on the road gradient, Δ, and the vehicle mass, m. The centre of gravity shifts during braking is not considered because the focus of the model is the highway where acceleration and deceleration are less important outside of rush hours.

2.1 Inputs Parameters of the Model

The forces acting on road vehicles depend on input variables related to three elements: (1) the vehicle, (2) the road, and (3) the weather (Table1).

Table 1: Input parameters of the model.

Input	Type:	Source
Drag coefficient	Vehicle	(Chowdhury *et al.*, 2013)
Frontal area of the vehicle		(Chowdhury *et al.*, 2013)
Vehicle and shipment weight		(Statistics Canada, 2019)
Maximum engine power		ADVISOR
The tire	Vehicle, road and weather	ADVISOR
Pavement type	Road	MTQ private database
IRI		MTQ private-historical survey
Road grade		MTQ private-historical survey
Speed limit		MTQ private database
Pavement temperature	Road and Weather	Calculated (Khan *et al.*, 2019)
The air temperature	Weather	(CWEEDS, 2021)
Solar radiation		(CWEEDS, 2021)
Relative humidity		(CWEEDS, 2021)
Wind speed and direction		(CWEEDS, 2021)

During each simulation, the variable related to the vehicle and weather stay constant unless the nearest weather changes on the simulated route. However, the information related to the road varies and come from various sources (Table 1). For the simulation purpose, the road-related data are collected and resampled into homogenous segment of 100-m long. Missing pavement-type data are replaced with the value “asphalt” which is the most common surface in Canada or “mix” (concrete covered by a layer of asphalt) for road structures such as overpasses and bridges. Missing IRI data are replaced with the average value for the road type and surface. Missing road grades are interpolated with the previous and next points. Speed limits are assumed to remain constant between the changes in the dataset.

2.2 Simulation Algorithm

Figure 2 presents the algorithm used to calculate the speed profile and the energy consumption. The algorithm includes a predictive control loop that generates a speed profile mimicking a typical driver behavior. It predicts the difference between vehicle speed and the speed limit on a certain distance on the simulated route and modify the traction force to remain as close as possible to the speed limit. The generation of speed profile is important because the vehicle does not always follow the speed limit. For instance, the truck speed can be limited by its engine power when travelling uphill. Drivers also tend to accelerate before driving up a steep slope or coast ahead of a descent.

Two model parameters define the driver behavior in the model: (1) the prediction time and (2) the weight the driver is giving to the events that happen in the predictions. In average, a truck driver reacts to an event around 18 seconds in advance (Thijssen *et al.*, 2014). For the controller design, it was assumed that at least 50 percent of a driver’s decisions are made on an event that

happens before 18 seconds. Consequently, a 60-second prediction time was selected along with a normalized exponentially decreasing weighting function with half of its area included within the average prediction time (18 seconds). This weighting can be changed to represent different driver behavior. By giving more importance to the nearer future, the driver is more aggressive as it is forced to react spontaneously to events occurring on the road.

At each simulation time, the driver-algorithm predicts the vehicle's speed for the duration of the prediction time as if the traction force remains constant. The error between the predicted speed and the speed target (limit) of the road is calculated for the duration of the prediction. For instance, the error will increase if the vehicle accelerates due to a decrease in the road grade or to a speed-limit drop. The predictive controller computes a variation in traction force, ΔF_t, by integrating the error and multiplying the result with the weighting function, w_i,:

$$\Delta F_t = K \sum_{i=0}^{T_p} (v_i - v_{ri}) w_i \Delta t \tag{1}$$

where K is a gain, T_p is the prediction time, v_i and v_{ri} are respectively the vehicle speed and the target speed at the instant i in the prediction, and Δt the controller sampling time.

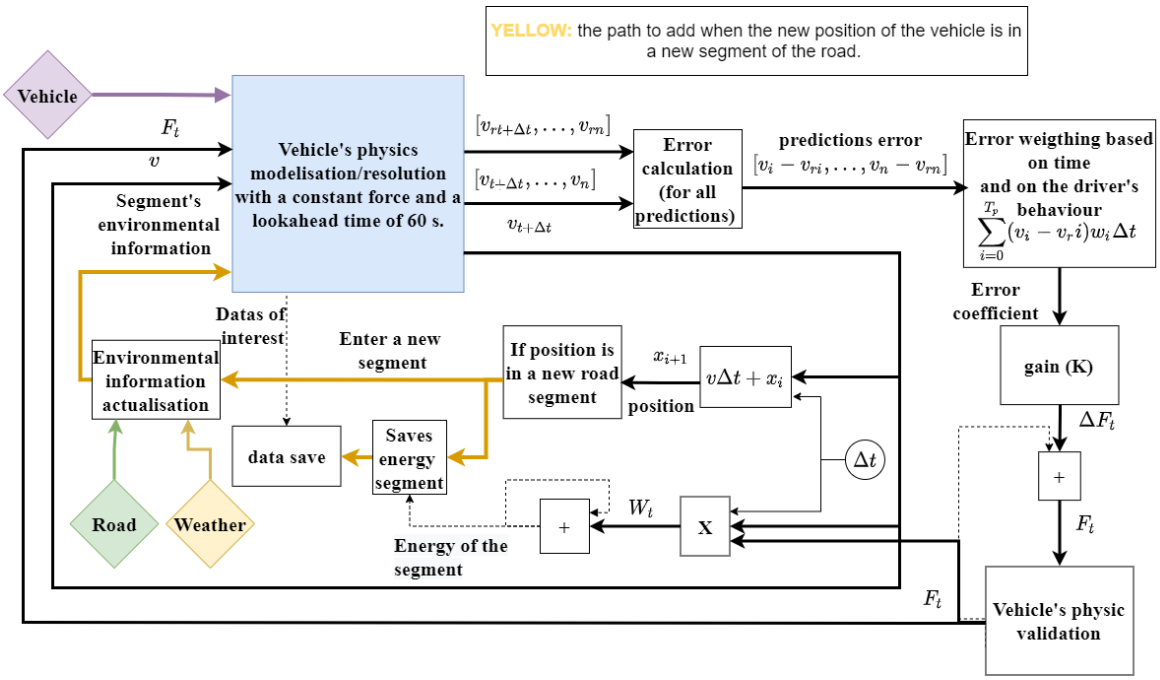

Figure 2: Block diagram of the simulation algorithm where v is the speed of the vehicle relative to the wind speed, v_r is the target speed (limit) of the vehicle, W_t is the work done by the traction force, x is the position of the vehicle, F_t is the traction force of the vehicle.

The algorithm also ensures that the total traction force (sum of actual force and variation) follows the physical limits of simulated truck. The power required for the new traction force is calculated and compared to the maximum power of the truck to ensure that such force is physically possible. If the maximum is reached, the new traction force is limited to the

maximum traction force under the simulated conditions. The speed generated by the new traction force is also calculated to verify if the truck's speed respects Quebec (Canada) strict speed limit for trucks of 105 km/h. Since 2009, a law imposed the activation of a speed limiter at 105 km/h for all trucks equipped with such technology (Ministry of Transportation of Quebec, 2009). To reflect the behavior of truck drivers, this 105 km/h limit is used in the simulation even though the maximum speed limit on Quebec motorways is ironically 100 km/h. To mimic truck maximum torque without simulating the gear system, the acceleration is limited at 0.4 m/s^2 (Bokare & Maurya, 2017) until the engine power becomes the limit of the acceleration.

The distance travelled and the energy consumed by the vehicle computed on a time-based interval is resampled into 100 m homogenous segments. To do so, when the vehicles enter a new homogenous road segment, the energy consumption of the segment is georeferenced as a line and linked to a map. The road properties of the new segment replace the previous segment. In any cases, a new loop starts. The complexity level of the vehicle simulation can vary. For instance, the vehicle simulation does not model the gear systems but assumes the engine power are constant (Minaker, 2019).

The vehicle's physics modelling/resolution is not detailed in Figure 2 as the model can be adjusted to fit the needs. However, the new speed is calculated by solving Newton's second Law on the vehicle:

$$m\frac{dv}{dt} = F_t - mg\left(\Delta + c_r\right) - \frac{1}{2}\rho A c_d \left(v - v_w\right)^2 \tag{2}$$

Where c_d is the drag coefficient, m is the mass, F_t is the traction force, g is the gravitational constant, c_r is the rolling resistance coefficient, ρ is the air density, A is the frontal area of the truck, v_w is the relative wind speed and Δ is the road grade. The small-angle approximation is used as highway inclination gradient is rarely above 10%. This ordinary differential equation is solved using Runge-Kutta method.

Each parameter in the Equation 2 can be constant or calculated by a model during each closed loop iteration. In other words, each parameter can be approximated by a more specific and detailed model. For the project on rolling resistance commissioned by the MTQ for instance, the MapEUR used a relatively complex model to approximate the rolling resistance coefficient which needs to be calculated during each iteration loop. This model is detailed in section 2.3 and some results of the simulations are shown as a case study in section 3.

Another important feature of the MapEUR is that it can display all sorts of results including the different results calculated by an incorporated model. For instance, it can save the different energy losses (*e.g.* aerodynamic, rolling resistance), the potential energy, the power used by the motor and the total energy consumed by the vehicle.

2.3 Model of Rolling Resistance

The rolling resistance model in the MapEUR is divided in three independent categories of phenomenon: (1) the viscoelastic deformation of the tire, (2) the road roughness and (3) the viscoelastic deformation of the road structure. The last category is often called Structure-

induced Rolling Resistance (SRR) (Chupin et al., 2013). The total rolling resistance is the sum of the contribution of each category.

The effect of tire viscoelasticity on rolling resistance depends on many parameters such as: vehicle speed, tire temperature, pressure in the air chamber, tread depth, etc (Sandberg *et al.*, 2004). For a given vehicle speed, there is a corresponding steady-state tire temperature. As the specific aim of this case study is to evaluate the effect of road-induce rolling resistance, we supposed that the tire pressure remains constant throughout the year, the vehicle speed does not significantly vary. Therefore, the coefficient of rolling resistance related to the tire remains constant. The presented model uses a typical rolling resistance value of 0.005 representing a modern heavy-vehicle tire (Madhusudhanan *et al.*, 2021).

The road roughness is commonly quantified with the International Roughness Index (IRI). The contribution of road roughness to rolling resistance can be estimated with the IRI and the waviness number, which is the slope of the power spectral density of the road profile in a logarithmic scale (Louhghalam *et al.*, 2015). By representing the dynamic properties of the truck with a quarter-car model, it is possible to use the random-vibration theory to estimate the root mean square value of suspension motion, which directly corresponds to an increase in rolling resistance. For a sprung mass of 34.9 tons and a waviness number of 2.41, the relation between roughness rolling resistance force and the IRI is (Louhghalam *et al.*, 2015):

$$F_{IRI} = 17.933\mathrm{IRI}^2 + 3.8984\mathrm{IRI} - 2.1831 \tag{3}$$

Finally, the SRR mainly depends on the pavement material, the foundation of the road, the thickness of the pavement and the pavement temperature (Bazi *et al.*, 2020; Chupin *et al.*, 2013). For rigid pavement (*e.g.* concrete), the SRR contribution is almost negligible and is independent of experimental conditions. Its value represents approximately 15 N for a 40-ton (40,000 kg) truck (Bazi *et al.*, 2020). For a soft pavement (*e.g.* asphalt), the SRR force of a 40-ton truck is defined by an exponential regression on some results interpolated from different sources *(Bazi et al.*, 2020; Chupin *et al.*, 2013):

$$c_{SRR} = \frac{8.574e^{0.07682\mathrm{T}_p} + 9.354}{40,000g} \tag{4}$$

Where T_p is the pavement temperature in °C and g the gravitational constant. Equation 4 represents a pavement thickness of 0.274 m and a modulus of elasticity of the sub-grade of 50 MPa.

The pavement temperature was estimated the 24-h model without wind direction developed by Khan *et al.* (2019). It is a regression model based on meteorological and pavement surface temperature measurements over one year. The model inputs are the air temperature, the solar radiation, the relative humidity and the wind speed. It was assumed that the temperature in the pavement was uniform, and rain or snow have no effect on the pavement temperature.

3. Case Study Results

This section presents how the MapEUR can be used through a case study taken from a research project with the MTQ (Ministry of Transportation of Quebec, Canada). The aim of this project was to assess the effect of pavement type on heavy-vehicle fuel consumption in the context of the Canadian climate which varies from -30°C in winter to 30°C in summer. These significant temperature variations affect the viscoelastic properties of the pavement and therefore can play a significant role in the fuel consumption of heavy vehicles.

The presented results show a preliminary evaluation of this effect on the structure-induced rolling resistance (SRR) and heavy-vehicle fuel consumption over a year. To do so, we have simulated the journey of a typical truck travelling the same route once a week for one year. Each simulation used the weather data of Wednesday 14h00 (taken arbitrarily) from September 2019 to October 2020. The vehicle properties are the following: a maximum power at the wheel of 335 kW (450 hp), a gross mass of 38,000 kg, a frontal area of 8.6 m^2, a drag coefficient of 0.7 and an average efficiency of 39%. The route presented was selected because there is an interesting variation of road grade, IRI, pavement and speed limits.

3.1 The Average Speed Profile over a Year

Figure 3 presents the speed profile generated by the algorithm. The speed profile changes with the variation of the road grade. For example, when the road grade varies between -2% and 2%, the vehicle speed varies between 100 km/h and 105 km/h. The effect of the predictive controller can be seen at 17 km where the vehicle accelerates above the speed limit before an important road grade. The speed then decrease due to the slope that averages an inclination gradient of 4.8% over 1 km, which represents a normal behavior for the modeled truck (Lan & Menendez, 2003). Another example where the algorithm anticipates a speed-limit change is at around 75.5 km where vehicle's speed decreases almost 2 km before a highway exit where the speed limit goes from 105 km/h to 55 km/h.

The anticipation of the driver model is also visible in Figure 3 b) where the power decrease before a downhill to limit the acceleration (*e.g.* at 17 km). Note that a negative percentage of the maximum power used represent the power used for braking. For downhills below -2% of slope, the truck power tends to be negative. This is normal considering the law in Quebec (Canada) that forces the truck that have a speed limiter to activate it at 105 km/h. The speed limiter incorporated in the model can be adjusted to fit the regulation of the simulated road. Note that the driver only uses its brake when he needs to brake more than the engine-retarder system can. For the modelled truck, the engine-retarder system can break up to half the motor power as it require a motor torque of 600 N with a gear ration of 4:1 (Ye *et al.*, 2011). With that information, the driver only brakes in the middle of long slopes. When the gradient increase, more power is used by the truck to fight that gradient. The only places the truck is at maximum power is just before or during the climbing of a steep slope. The highest fuel consumption was 133 L/100km at the end of the 1-km slope that averages 4.8%. During this climb, the fuel consumption continued to increase as the speed decreased while using maximum power. The average fuel consumption of whole the journey was 34.7 L/100 km.

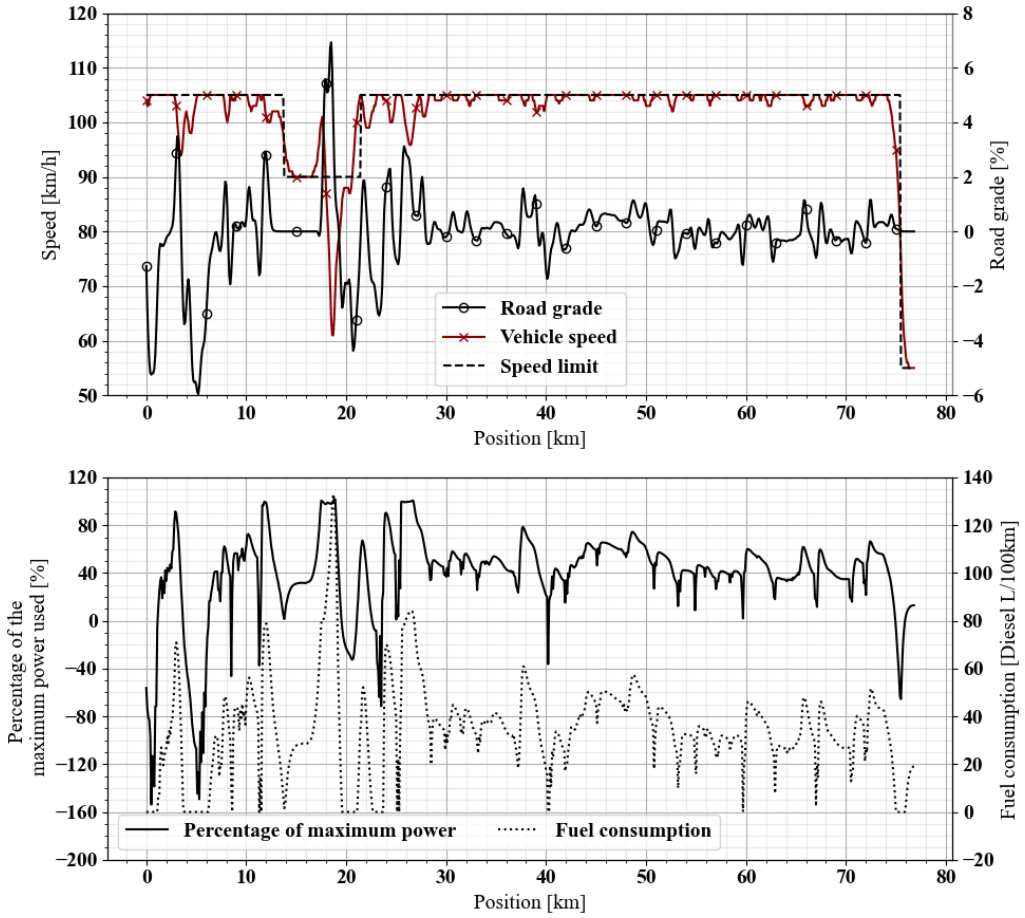

Figure 3: a) Speed profile of a typical semitrailer truck with a maximum power of 335 kW, a gross mass of 38,000 kg, a frontal area of 8.6 m^2, a drag coefficient of 0.7 on the simulated route near Quebec City; b) Percentage of the maximum motor power used and vehicle fuel consumption during the simulated route.

3.2 The Mapped Energy Consumption

One of the main purposes of the MapEUR is to display the data shown in Figure 3 directly on a map to help the policy and decision makers to understand what is happening on their roads. A typical map is presented in Figure 4. This figure shows for instance that the highest energy density is during the 1-km slope at 18 km. With that knowledge, a company could decide to locate their distribution centre in a sector that avoid this slope, or logistic operators could try to find a slighly longer route that avoid that slope in order to reduce its fuel consumption. Policy makers could also select the best location to place and test different electrification solutions for highways. The figure also shows that the lowest consumption of energy are when the vehicle is going down a slope at the speed limit (at 6 km) or when the speed is reduce to 55km/h as the drag becomes significantly less important (at 75 km). Another interesting piece of information provided by the map, is that it can predict the maximum speed of different truck on higway slope and identify all the existing slopes that need to be evaluated for the addition of slow-climbing lanes in order to reduce trafic jams

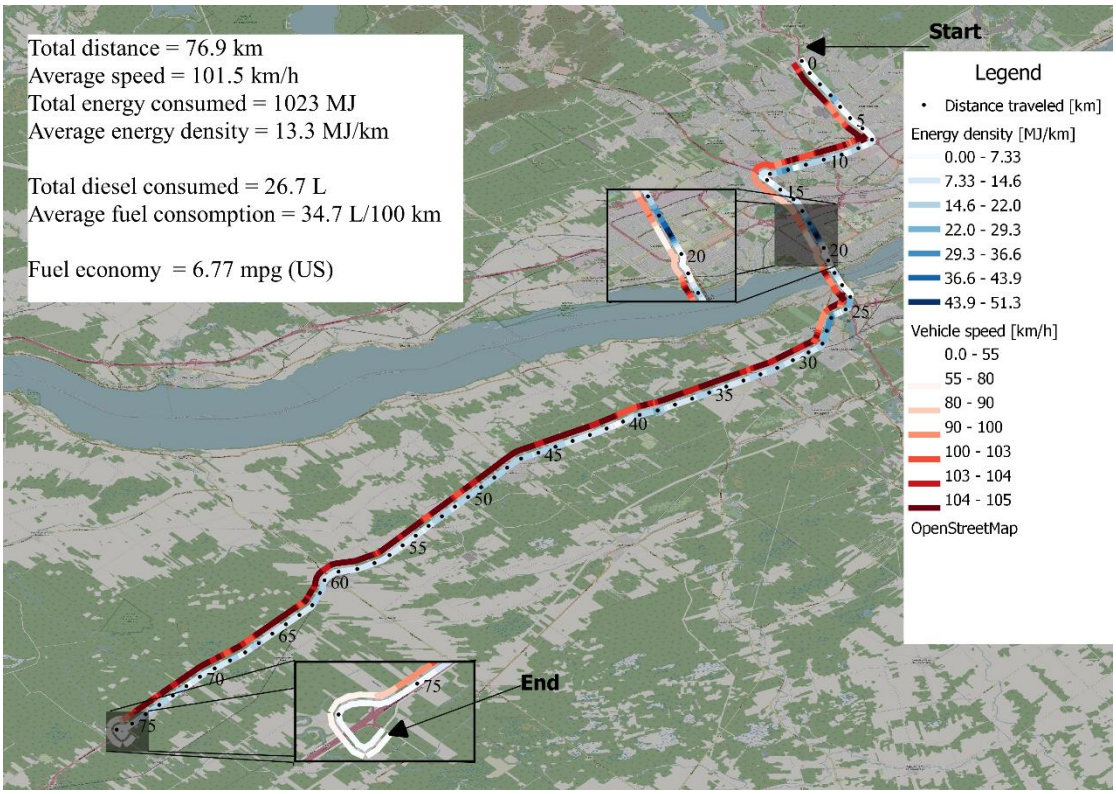

Figure 4 : Average speed profile and average energy consumption of all 52 simulations with a 38,000-kg truck with a frontal area of 8.6 m^2, a drag coefficient of 0.7 and a maximum power of 335 kW.

4. Discussion and Future Works

The presented algorithm calculates the energy of a vehicle's route by calculating the speed profile of that vehicle. The driver model used in the algorithm can anticipate future events like steep slopes by accelerating before climbing them. It also start reducing its speed a few kilometers before a drastic change of speed limit (105 km/h to 55km/h) as would a normal driver do. The algorithm reproduced well the reduction of speed when a truck climbs a long and steep slope. The driver model keeps most of the time the vehicle speed near the simulated speed limit. The speed profile generated by the algorithm reprents well a typical heavy-vehicle drive cycle. A probabilist approach needs to be used to improve the statistical significance of the model where different driver behaviors (more and less predictive) can be modelled. This level of modeling based on real data analysis will be part of future works on the MapEUR.

For the simulated route, the average consumption over the year was 34.7 L/100 km which is representative of typical trucks (Nylund & Erkkilä, 2005). In addition, the drag losses, the rolling resistance energy losses and the constant engine efficiency have been validated with ADVISOR (T. Markel *et al.*, 2005). As computing speed is critical for the MapEUR, it is not expected to include an engine map and gear-shifting model. The constant efficiency hypothesis will be keep but improve in future works by statistically including the efficiency variation based the vehicle mass and type.

Presenting the results directly on a map can help people less familiar with vehicle physics to understand and analyse the implication of the road network on fuel consumption. The map helps to identify and quantify the highest energy density sectors of a road network. That functionnality gives the MapEUR a myriad of usages based on the different simulated scenarios. The MapEUR can also evaluate the climate impact by simulating and comparing the energy consumption of different times of the year. It can also evaluate the total consumption of a certain period of time by simulating the different vehicles. These last two functionnalities could help policy makers establish new policies designed for different times of the year to reduce GHG emissions.

The traffic is not completly incorporated in the model yet. The traffic will be modelled by using a Monte-Carlo Simulation with different truck archetypes, different time of the year, different weather based on statistical data, and different driver behaviours. It will also include the likeliwood of traffic slowing down or jamming for different roads and moment of the day. The Monte-Carlo analysis will represent a more accurate picture of the heavy-vehicle energy consumption as it will consider the different types of heavy-vehicle, the traffic, and the weather.

5. Conclusion

The MapEUR models energy consumption of trucks based on their specific speed profile. The speed profile is generated with a driver model that anticipates variations of speed limit and road grades. The results are presented directly on a road map. These energy maps are easy to understand, and they can help policy makers to analyze the impact of green technologies on vehicle emissions. The vehicle, road and weather statistics are available for the major roads in the province of Quebec in Canada which enable a relatively accurate estimation of truck GHG emissions with a maximum error of 3.6% for a truck modeled on highway when compared to the results of ADVISOR (T. Markel *et al.,* 2005). The weather database used in the MapEUR enables an analysis of the impact of the climate on fuel consumption. The modularity of the tool structure enables to change the underlying hypothesis and analyze specific parameters of vehicle physics. For example, a complex rolling-resistance model based on pavement type and the weather was added to the simulation for a study commissioned by the MTQ to evaluate the impact of different road pavement surfaces on energy consumption. The tool can be adapted to the precision required to analyze different decarbonizing solutions and strategies. In the future, traffic modelled based on Monte-Carlo simulations will be used to quantify the energy consumed by a road over a year.

6. References

Ainalis, D. T., Thorne, C., & Cebon, D. (2020). White Paper Decarbonising the UK ’s Long-Haul Road Freight at Minimum Economic Cost. *The Centre for Sustainable Road Freight*, *July*. http://www.csrf.ac.uk/2020/07/white-paper-long-haul-freight-electrification/%0Ahttp://www.csrf.ac.uk/wp-content/uploads/2020/07/SRF-WP-UKEMS-v2.pdf

Bazi, G., Hajj, E. Y., Ulloa-calderon, A., Ullidtz, P., Bazi, G., & Hajj, E. Y. (2020). Finite element modelling of the rolling resistance due to pavement deformation. *International Journal of Pavement Engineering*, *8436*. https://doi.org/10.1080/10298436.2018.1480778

Bokare, P. S., & Maurya, A. K. (2017). Acceleration-Deceleration Behaviour of Various Vehicle Types. *Transportation Research Procedia*, *25*, 4733–4749. https://doi.org/10.1016/j.trpro.2017.05.486

Chowdhury, H., Moria, H., Ali, A., Khan, I., Alam, F., & Watkins, S. (2013). A study on aerodynamic

drag of a semi-trailer truck. *Procedia Engineering*, *56*, 201–205. https://doi.org/10.1016/j.proeng.2013.03.108
Chupin, O., Piau, J.-M., & Chabot, A. (2013). Evaluation of the Structure-induced Rolling Resistance (SRR) for pavements including viscoelastic material layers. *Materials and Structures*. https://doi.org/10.1617/s11527-012-9925-z
CWEEDS. (2021). *Canadian Weather Energy and Engineering Datasets (CWEEDS)*. https://climate.weather.gc.ca/prods_servs/engineering_e.html
ECCC. (2020). Greenhouse Gas Emissions- CANADIAN ENVIRONMENTAL SUSTAINABILITY INDICATORS. *Encyclopedia of Soils in the Environment*, *4*, 145–153. https://www.canada.ca/content/dam/eccc/documents/pdf/cesindicators/ghg-emissions/2020/greenhouse-gas-emissions-en.pdf
International Transport Forum. (2010). *Transport Greenhouse Gas Emissions Country Data 2010*. http://www.internationaltransportforum.org/Pub/pdf/10GHGcountry.
Khan, Z. H., Islam, M. R., & Tarefder, R. A. (2019). Determining asphalt surface temperature using weather parameters. *Journal of Traffic and Transportation Engineering (English Edition)*, *6*(6), 577–588. https://doi.org/10.1016/j.jtte.2018.04.005
Lan, C. J., & Menendez, M. (2003). Truck speed profile models for critical length of grade. *Journal of Transportation Engineering*, *129*(4), 408–419. https://doi.org/10.1061/(ASCE)0733-947X(2003)129:4(408)
Louhghalam, A., Akbarian, M., & Ulm, F.-J. (2015). Roughness-Induced Pavement–Vehicle Interactions. *Transportation Research Record: Journal of the Transportation Research Board*, *2525*(1), 62–70. https://doi.org/10.3141/2525-07
Madhusudhanan, A. K., Ainalis, D., Na, X., Garcia, I. V., Sutcliffe, M., & Cebon, D. (2021). Effects of semi-trailer modifications on HGV fuel consumption. *Transportation Research Part D*, *92*(February), 102717. https://doi.org/10.1016/j.trd.2021.102717
Ministry of Transportation of Quebec. (2009). *Speed limiter control measure*. https://www.transports.gouv.qc.ca/en/camionnage/Pages/limiteurs-de-vitesse.aspx
Mosaddeghi, F., & Oveisi, M. (2015). *Aerodynamic drag reduction of heavy vehicles using append devices by CFD analysis*. 4645–4652. https://doi.org/10.1007/s11771-015-3015-7
Nylund, N.-O., & Erkkilä, K. (2005). Heavy-duty truck emission and fuel consumption: Simulating real-world driving in laboratory conditions. *Proceeding of the 2005 DEER Conference*, 1–23.
Pevitt, C., Chowdhury, H., Moria, H., & Alam, F. (2012). *A computational simulation of aerodynamic drag reductions for heavy commercial vehicles Commercial Vehicles*. *January*.
Sandberg, T., Ramdén, C., & Gamberg, M. (2004). Tire Temperature Measurements for Validation of a New Rolling Resistance Model. *IFAC Proceedings Volumes*, *37*(22), 589–594. https://doi.org/10.1016/s1474-6670(17)30407-x
Statistics Canada. (2019). *Trucking commodity industry activities*. https://www150.statcan.gc.ca/t1/tbl1/en/tv.action?pid=2310021901
T. Markel*, A. Brooker, T. Hendricks, V. Johnson, K. Kelly, B. Kramer, M. O'Keefe, S. Sprik, K. W. (2005). ADVISOR: a systems analysis tool for advanced vehicle modeling. *Elsevier*, *50*(1), 107–114. https://doi.org/10.1016/j.lungcan.2005.05.006
Thijssen, R., Hofman, T., & Ham, J. (2014). Ecodriving acceptance: An experimental study on anticipation behavior of truck drivers. *Transportation Research Part F: Traffic Psychology and Behaviour*, *22*, 249–260. https://doi.org/10.1016/j.trf.2013.12.015
Ye, L., Li, D., Ma, Y., & Jiao, B. (2011). Design and performance of a water-cooled permanent magnet retarder for heavy vehicles. *IEEE Transactions on Energy Conversion*, *26*(3), 953–958. https://doi.org/10.1109/TEC.2011.2157347